Surface properties of the doped silica hydrophobic coatings deposited on plasma activated glass supports

Michał Chodkowski [1], Konrad Terpiłowski [1], Olena Goncharuk [2]

[1] Department of Interfacial Phenomena, Maria Curie-Sklodowska University in Lublin, M. Curie-Skłodowskiej 3, 20-031 Lublin, Poland

[2] Chuiko Institute of Surface Chemistry NASU, 17 General Naumov Str., Kyiv 03164, Ukraine

Corresponding author: michal.chodkowski@poczta.umcs.lublin.pl (Michał Chodkowski)

Abstract: The paper discusses preparation and characteristics of silica hydrophobic layers deposited on the plasma-modified glass supports. The surfaces were investigated using wettability measurements, profilometry, photoacoustic and infrared spectroscopy, X-ray photoelectron spectroscopy as well as scanning electron microscopy. The wettability measurements showed that the obtained surfaces are hydrophobic – the water contact angle was in the range of 140-150 degrees. The photoacoustic and infrared spectroscopy as well as X-ray photoelectron spectroscopy disclosed the surface compositions, particularly that of the hydrophobic alkyl groups deposited on them. They were methyl groups introduced during hydrophobization by hexamethyldisilazane. In addition, it was found that the number of groups on the surface depends on the kind of plasma by which the supports were activated. The optical profilometer showed differences in the surface roughness which affects their hydrophobicity. Moreover, the surface free energies were determined using the contact angle hysteresis method. They disclosed differences in each surface, depending on the way of supports activation. The largest hydrophobicity was obtained on the layer deposited on the support activated by the argon plasma. However, support activation by the air plasma resulted in a decrease of hydrophobicity compared to that of the non-activated surface.

1. Introduction

Silica is a common name of silicon dioxide of the chemical formula SiO_2. This is a group of minerals composed of the two most common elements in the Earth's crust: silicon and oxygen. Silica occurs in both crystalline and amorphous states but commonly it can be found in the former one. There are many naturally occurring silica minerals such as coesite, cristobalite, keatite, moganite, quartz, seifertite, stishovite, tridymite, chalcedony, jasper, opal or tiger's eye; synthetical forms such as fumed silica, silica gels, aerogels or fused quartz also exist. Thus, it is one of the most complex and abundant groups of minerals commonly applied in many branches of industry and as a structural material.

Silica gels are an interesting and future-oriented group of silica-based materials. They are composed of an irregular, three-dimensional framework of silicon and oxygen atoms which are connected by the siloxane bond ≡Si-O-Si≡. Such structure can be obtained by gelation from a silica precursor using the sol-gel process, which involves creation of polysiloxane network starting with soluble molecular precursors, typically silicon alkoxides – most commonly for the safety reason it is tetraethoxysilane - TEOS (Innocenzi, 2016), following the reaction of inorganic polymerization. The properties of the obtained product depend on the reaction conditions such as temperature, type of solvent (water or organic), catalyst, pH range or duration. This is a relatively simple, cheap, effective and flexible technology characterized by many advantages. Thus, it can be used for obtaining a wide range of materials (Milea et al., 2011). The Stöber process (Stöber et al., 1968) is the most common for this purpose. This is a variation of the sol-gel process which allows to obtain silica particles of controllable and

uniform size (Bogush et al., 1988) including modified silicas, for example with polyorganosiloxanes in the presence of dialkyl carbonates (Klonos et al., 2019; Protsak et al., 2017 and 2019) for various applications.

Coatings, films and thin layers on different substrates can be obtained based on the silica gel, for example by means of the dip-coating method (McDonagh et al., 1995). Additionally, the functional properties of the coatings can be changed by silica gels modification. This can be achieved modifying (doping or co-precursor adding) the gels or their surface. In this way hydrophobic silica can be obtained. It possesses hydrophobic groups, which are normally alkyl or polydimethylsiloxane chains, chemically bond to their surface ensuring water resistant properties and can be considered as a hydrophobic surface (Zhao et al., 2011). The surface hydrophobization is usually achieved by the reaction with aminosilanes possessing alkyl chains, for example hexamethyldisilazane, although new compounds are synthesized (Arase et al., 2019).

The silica gel modification is a very powerful method which was employed by both scientists and industry for various applications. This kind of silica can be used in biocatalytic applications by doping the silica gel with biomolecules (Pierre, 2019), production of durable, hydrophobic and oleophilic cotton fabric (Jiang et al., 2019), as well as superhydrophobic and flame-retardant coatings on cotton fabrics (Lin et al., 2019), construction of superhydrophobic coatings simulating the lotus leaf structure (Wang et al., 2019), production of hydrophobic coatings for aeronautical applications (Piscitelli et al., 2019), production of superhydrophobic organic-inorganic hybrid nanocomposite coatings (Zhi et al., 2019), synthesis of hybrid silica materials, such as antibacterial and biocompatible silica-chitosan coatings for implants (Palla-Rubio et al., 2019) and biohybrid ones for encapsulation of microorganisms (Ponamoreva et al., 2019), removal of heavy metals from water (Li et al., 2019) or as a sorbent (Sulejmanović et al., 2019) and filler for chromatographic columns (Ito et al., 2019).

Fabrication of the polysiloxane coatings using the sol-gel method with TEOS as a precursor in connection with other methods for the surface properties modification, such as doping with nanosilica particles, hydrophobization or plasma treatment of the support, makes it possible to obtain hydrophobic and superhydrophobic surfaces.

The aim of this paper was to obtain silica hydrophobic coatings on the glass supports activated by cold plasma. The surface properties of the layers were modified by the addition of nanoparticles and hydrophobization. The SEM, XPS and IR/PAS techniques were used in order to analyse the structure and composition of the films. Optical profilometers in combination with contact angle measurements were made in order to analyse the surface impact on the wettability and the surface free energies were compared in order to find changes in the surface properties depending on the way of glass supports activation.

2.   Materials and methods

2.1. Materials

The following reagents and materials were used during the experiment:
- acetone (99%, *POCH S.A.*, Poland);
- methanol, MeOH (99%, *POCH S.A.*, Poland);
- chloroform (98%, *POCH S.A.*, Poland);
- tetraethoxysilane, TEOS (98%, *Aldrich*);
- hydrochloric acid, HCl (35-38%, *POCH S.A.*, Poland);
- ethanol, EtOH (96%, *POCH S.A.*, Poland);
- hexamethyldisilazane, HMDS (98%, *Aldrich*);
- n-hexane (99%, *POCH S.A.*, Poland);
- glass microparticles (a finely ground quartz glass for the preparation of dental glass-ionomer cement with diameters from 0.95 to 1.2 µm);
- nanosilica, A300 (99.6% SiO_2, *Pilot Plant of Chuiko Institute of Surface Chemistry*, Ukraine);
- polydimethylsiloxane, PDMS 200 (*Kremniypolymer*, Ukraine);
- dimethyl carbonate, DMC (99%, *Aldrich*);
- glass plates (76x26x1 mm microscope slides, *Comex*, Poland);

2.2. Surfaces preparation

2.2.1. Supports preparation

The glass plates were washed in an ultrasonic bath containing acetone and methanol, then they were rinsed with the chloroform and dried at the ambient temperature. After cleaning the surfaces were activated by means of the *Pico* system from *Diener Electronic* (Germany) using cold plasma at low pressure. The sample was put into the apparatus chamber and the pressure was reduced to the value of 20 Pa. Subsequently, the gas (air or argon) was delivered into the chamber with the flow set at 20 sccm (standard cubic centimetre per minute) and the sample was treated by the plasma. The 40 kHz RF (radio frequency) generator powered by 230 V voltage was used with 500 W power and the process lasted 60 s. Finally, the chamber was flushed with the air for 10 s in order to blow out the remained gaseous products and vented to obtain the atmospheric pressure inside. In this way, the supports activated by air plasma and argon plasma were prepared.

2.2.2. Filler synthesis

Glass microparticles (40 g) and nanosilica A300 (4 g) were placed in a beaker with a stirrer. Then 1 cm^3 of ethanol was added while stirring for 600 s. Then, the mixture composed of PMS200 (1.2 g) and DMC (1.2 g) was added dropwise, and the composition was still being stirred at room temperature for 3600 s. Then the product was heated at 373.15 K for 3600 s and at 473.15 K for another 3600 s. Finally, the filler suspension in ethanol with a concentration of 0.22 g/cm^3 was prepared. The ratio of the components of the suspension for coating with filled particles was experimentally selected based on the optimal combination of such characteristics as the viscosity of the suspensions, their colloidal stability and concentration of particles sufficient to obtain a uniform surface coating.

2.2.3. Coating synthesis

The hydrophobic silica coating was synthesised by the sol-gel method (Stöber process) using TEOS as the precursor and HCl as a catalyst of the hydrolysis. A ratio of $1.0:4.6\cdot10^{-2}:3.45$ was used for the TEOS:HCl:H$_2$O mixture and it was stirred for 7200 s at room temperature. Then the filler suspension in EtOH with the volume ratio 1:3 was added and the stirring was continued for 1800 s.

2.2.4. Coating applications

The glass supports were covered by the dip-coating. Then the substrates were kept in an exsiccator under HMDS (5% solution in hexane) vapour at ambient temperature and pressure for 86400 s in order to impart the surface hydrophobicity. Next the by-product (NH$_3$) and the unbound modifier were removed by heating the plates at 40°C for 7200 s. In this way three samples were obtained: coating deposited on the non-activated, argon and air plasma activated glass support.

2.3. Wettability measurements

Millipore Milli-Q ultrapure water contact angle measurements at the temperature 293.15 K ± 1 K were made in order to examine wettability of the obtained surfaces. The *DigiDrop Contact Angle Meter* (GBX, France) apparatus was used to measure the contact angles. It is equipped with a closed, thermostated chamber, video system and PC with the suitable software *WinDrop++*. Using the tilting plate technique, the measurements were made as follows: a water droplet of 6 µl volume was carefully settled on the given sample in the apparatus measuring chamber. Then the stand of the apparatus started to slope, and the droplet was filmed until it started to slide. Analysing the image frames of the droplets one frame was selected just before the droplet started to slide. Indication of droplet baseline, three-phase contact points and height of the examined droplet was necessary. Based on them, using the polynomial algorithm and the NURBS (non-uniform rational basis spline) model, the program computed the receding contact angle on the droplet front and the advancing contact angle on its rear. In this case, 10 water droplets were measured and averaged on each surface.

2.4. Topography and roughness

A *ContourGT 3D* Optical Profiler (*Bruker*, Germany) was used to measure the surface roughness and obtain information about the surface topography. The optical profilometer allows for contactless

analysis of any surface. The roughness parameters such as the arithmetic average of the absolute values of the roughness profile (arithmetic mean roughness, R_a) and the root mean square average of the roughness profile (root mean square roughness, R_{RMS} or R_q) were calculated based on the measurements for surface roughness characterisation.

2.5. Photoacoustic and infrared spectroscopy

The Fourier-transformed photoacoustic infrared spectra (FTIR/PAS) of the examined samples were recorded by means of *Bio-Rad Excalibur FT-IR 3000 MX* spectrometer over the 4000-400 cm^{-1} range at room temperature with the resolution 4 cm^{-1}, mirror velocity 2.5 kHz and maximum source aperture, using the *MTEC Model 300* photoacoustic cell. Dry helium was used to purge the photoacoustic cell before data collection. The spectra were normalized by computing the ratio of a sample spectrum to that of a MTEC carbon black standard. The sample was placed in a stainless-steel cup (diameter 10 mm) and the interferograms of 1024 scans were averaged for the spectrum, providing a good signal-to-noise (S/N) ratio. No smoothing functions were used. All spectral measurements were performed at least in triplicate.

Attenuated Total Reflection – Fourier Transform Infrared (FTIR-ATR) spectra of the obtained surfaces were recorded using *Nicolet™ iS10* FTIR Spectrometer equipped with the *Smart™ iTX* adapter. This single-bounce attenuated total reflectance device with the monolithic diamond provides the high-quality spectral data which allows material identification and verification. The spectra were recorded at room temperature over the 4000-400 cm^{-1} range with the resolution 4 cm^{-1} at least twice.

2.6. X-ray photoelectron spectroscopy

An UHV (Ultra High Vacuum) multi-chamber analytical system made by *Prevac* (Poland) with the *Scienta MX 650* (*Gammadata Scienta*) monochromatic X-ray source equipped with the Kα-Al anode and *R4000* hemispherical electron energy analyser were used in order to investigate quantitative and qualitative composition of the surface layer.

2.7. Scanning electron microscopy

A *Quanta™ 3D FEG* scanning electron microscope was used to obtain the surface morphology images. This is the high-resolution (1 nm at 30 kV), high-vacuum (up to $6 \cdot 10^{-4}$ Pa) system for 2D and 3D material characterization and analysis. The images were made at the pressure about $2 \cdot 10^{-4}$ Pa (high-vacuum mode) with the Au/Pd conductive coating sputtered and the accelerating voltage for the electrons (beam energy) was equal to 5.0 kV.

2.8. Surface free energy determination

The surface free energy (SFE) of each surface was calculated using the CAH (contact angle hysteresis) method proposed by Chibowski (Chibowski, 2003; Chibowski, 2007) in order to compare properties of the obtained layers. The advancing and receding contact angles averaged from the 10 measurements were used.

3. Results and discussion

The results of the surfaces wettability measurements are presented in the table below. In all cases, the obtained surfaces can be classified as hydrophobic because of the water contact angle (WCA) greater than 90°. Furthermore, they can be defined as highly hydrophobic surfaces (WCA > 120°). This type of surface should have a low surface free energy. The most hydrophobic coating is deposited on the support activated by the argon plasma, and the lowest contact angle is present in the case of a coating deposited on the support activated by air plasma. This may be the result of introducing hydrophilic groups on the support surface during activation with air plasma. These groups caused a worse surface coating by the gel during dip-coating.

The largest sliding angle can be observed on the layer deposited on the support activated by the air plasma. This is the result of incomplete coverage of the support surface and random heights (see below). Due to that the water droplet comes to stand on them. It is also the least hydrophobic of those obtained.

Worth noting is the fact that the most hydrophobic surface does not possess the smallest sliding angle. As it is indicated by the highest contact angle hysteresis, this may be a result of large energy heterogeneity of this surface. Thus, the layer deposited on the non-activated support is characterized by the best self-cleaning properties.

Table 1. Water wettability measurements of the surfaces

Support modification	Advancing contact angle (°)	Receding contact angle (°)	Contact angle hysteresis (°)	Sliding angle (°)
non-activated	145.2 ± 2.1	125.3 ± 2.5	19.8 ± 4.2	16.5 ± 1.6
argon plasma	147.0 ± 3.3	125.7 ± 2.6	21.2 ± 5.5	20.3 ± 2.3
air plasma	140.7 ± 3.1	135.4 ± 4.0	5.3 ± 2.8	25.4 ± 1.9
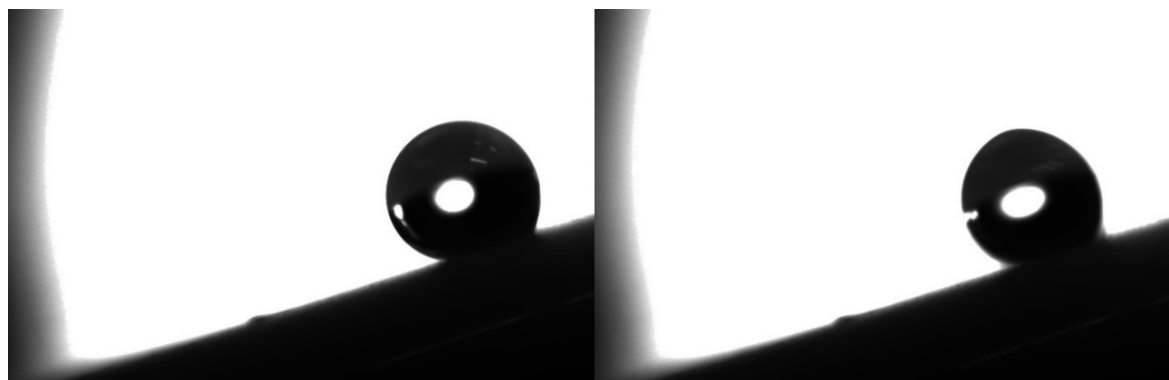
Fig. 1. Measurements of the coating on the non-activated support by the tilting plate method. In the right picture the droplet starts to slide so the left frame should be taken for the contact angles calculations

The lowest contact angle hysteresis occurs on the surface created on the support activated by air plasma which has also the largest sliding angle. It should be born in mind that there are many factors affecting the contact angle hysteresis on a given surface, including adhesion, roughness, and heterogeneity. However, they confirm that the ability of a drop to move along a surface is determined by the contact angle hysteresis (McHale et al., 2004).

The surface height maps and the surface profiles along the x-axis for each coating obtained by the optical profilometry are shown below. As it can be seen in Figs. 2 and 3, for the surface obtained on the non-activated and activated by air plasma support the roughness parameters are quite similar. On the non-activated support R_a is equal to 0.692 μm and R_{RMS} is equal to 0.985 μm while on the support activated by air plasma R_a is equal to 0.695 μm and R_{RMS} is equal to 0.973 μm.

Whereas for the surface obtained on the support activated by argon plasma R_a is also similar – it is equal to 0.672 μm, R_{RMS} equal to 0.883 μm is lower than the previous ones. This is reflected in the surface height maps in Fig. 4 – in the case of the surface on the support activated by argon plasma there is better coating coverage and simultaneously there are fewer random peaks and valleys which affects the R_{RMS} more than R_a. For this reason, this surface is the most hydrophobic. Moreover, comparing the surface maps, it can be concluded that modification of the support by air plasma causes worse coating coverage while its modification by argon plasma causes better coating coverage in reference to the unmodified one. This is also confirmed by the wettability measurements results.

The FTIR/PAS and FTIR-ATR spectra of the obtained surfaces were made in order to compare the composition of their top layers. They are shown in the figures below. The FTIR-ATR spectra (Fig. 5) exhibit peaks in the 700-1200 cm^{-1} region. The absorption in the 1000 to 1200 cm^{-1} region is due to the asymmetric stretches of the siloxane (≡Si-O-Si≡) groups; while the band located at about 800 cm^{-1} shows their bending vibrations. The more branched and longer the siloxane chain is, the broader and more complex the bands are. As it can be observed there, in some cases even two or more overlapping bands can appear. This confirms the basic structure of the coating composed of silica gel (polysiloxane), but does not show any hydrophobic groups on the surface. This is a result of pressing the ATR crystal to

the surface which destroys the top layer. Therefore, this method is not optimal for analyzing the surface of this type of samples. A better choice is the FTIR/PAS technique that does not destroy the top layer.
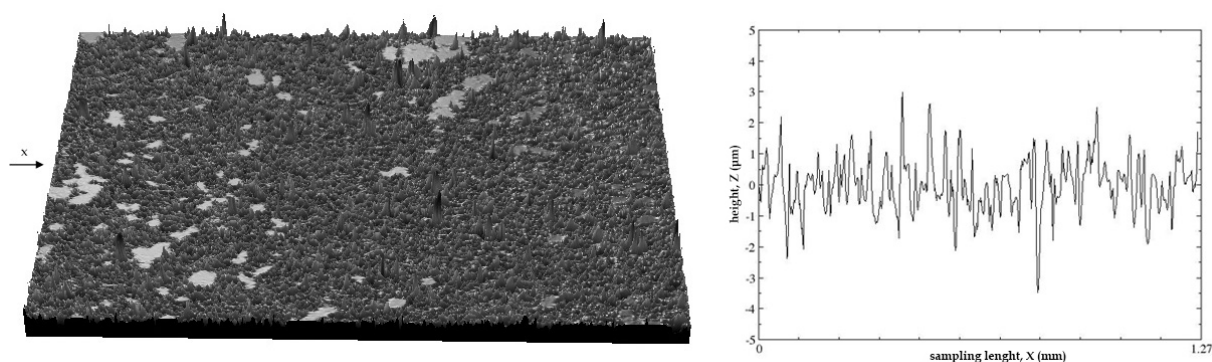
Fig. 2. The height map and the profile of the surface of the layer deposited on the non-activated support
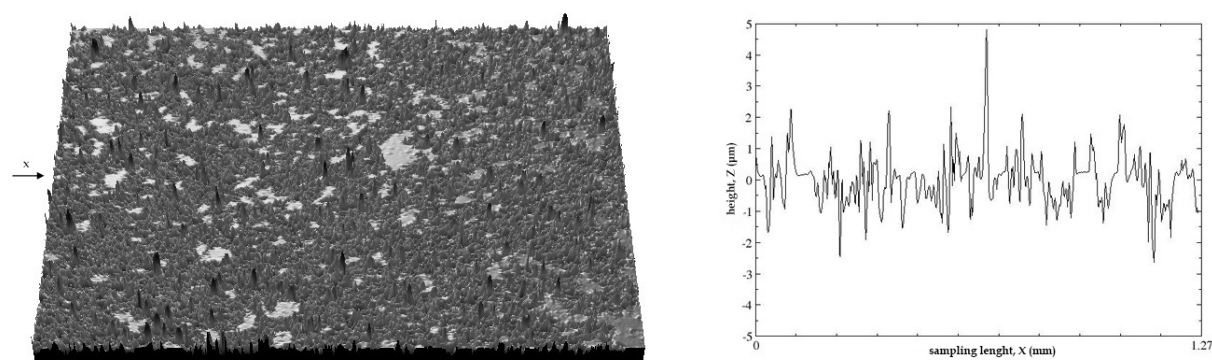
Fig. 3. The height map and the profile of the surface of the layer deposited on the support activated by air plasma
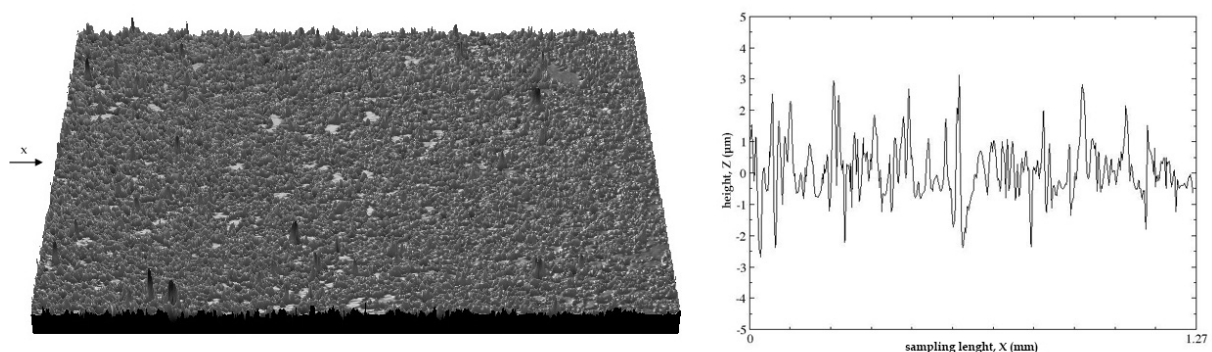
Fig. 4. The height map and the profile of the surface of the layer deposited on the support activated by argon plasma

As it can be seen in Fig. 6, the FTIR/PAS spectra exhibit peaks also in the 2850 to 3000 cm⁻¹ region. The bands correspond to the stretching vibrations of the C-H bond in the methyl groups which were introduced during the surface hydrophobization with hexamethyldisilazane. There are fewer methyl groups on the layer deposited on the support activated by air plasma. This confirms the least hydrophobic nature of this surface – it has the lowest value of the water contact angle of those fabricated. Additionally, the bands associated with the Si-O in-plane bending (rocking) in the 455 cm⁻¹ region can be observed.

In the case of the layer deposited on the support activated by air plasma, there is lower intensity of the band originating from the polysiloxane chains. This suggests worse deposition of the coating on this support.
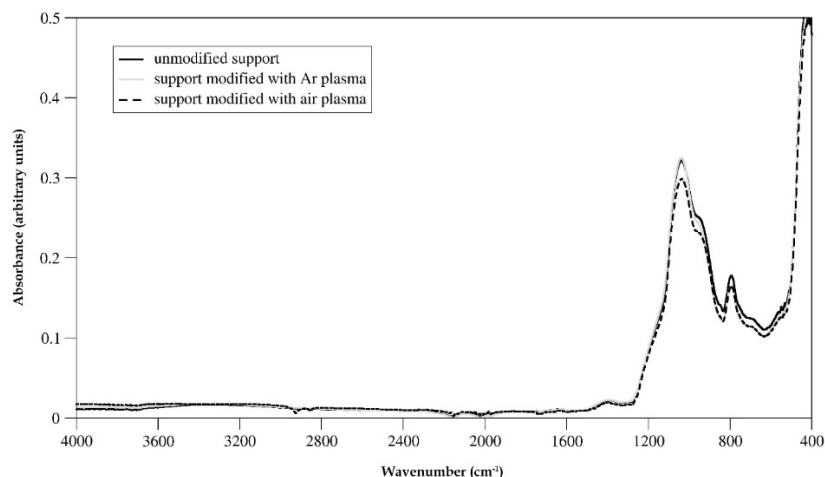
Fig. 5. The FTIR-ATR spectra of the surfaces
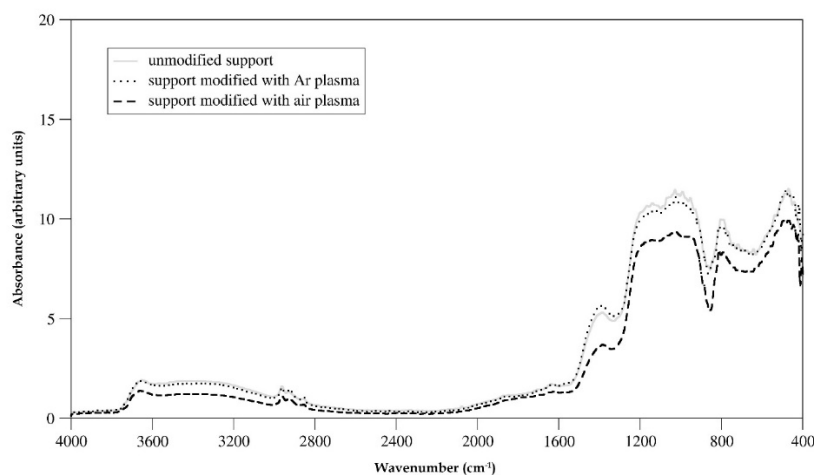
Fig. 6. The FTIR/PAS spectra of the surfaces

The scanning electron microscopy images are given below. In all the images specific structures created on the surfaces can be observed. As it is shown in Fig. 7, the glass microparticles, which were used as the filler, have been built into the silica system. As a result, nano- and microstructures on the surface were created. Those structures cause roughness of the surface and thus affect its wettability. Moreover, the surface roughness observed in the micro and nano scales can lead to obtaining the hierarchical structure which plays a key role in causing superhydrophobicity of surfaces.

Additionally, areas of the uncovered support can be observed on the surfaces. Considering the wettability of glass, which is hydrophilic, it may lead to obtain a hybrid surface, composed of hydrophobic and hydrophilic domains. However, an environmental scanning electron microscopy imaging must be done in order to confirm this property. This experiment allows observation of the condensation of water droplet on the surface under the saturated vapour conditions.

The XPS provides valuable information about quantitative and chemical compositions of the surface. As it can be seen in Table 2, in the case of the coating deposited on the support activated by air plasma, there is the smallest silicon amount with the relatively large oxygen content. This suggests the presence of oxygen-containing groups on the surface. They may be hydroxyl ones remaining after incomplete surface hydrophobization or other functional groups introduced by air plasma activation of the support. The carbon content is the largest but it should be considered in relation to that of other elements. However, in the case of the layers deposited on the other supports, the differences are less significant.

The surface free energy of the coating deposited on the support activated by argon plasma and the non-activated one has similar values. This is reflected in the contact angles which are also similar for

these surfaces. It can be concluded that activating the support by argon plasma caused a decrease in the surface free energy of the deposited coating; however, this is a value within the limits of the measurement (observational) error. The layer deposited on the support activated by air plasma has almost a double surface free energy value compared to that of the others. The SFE calculations were based on the water contact angle measurements; in the case of this method, the presence of polar (hydrophilic) groups on the surface will change the obtained values significantly. Such groups are oxygen-containing ones due to stronger interactions with the probe liquid (van der Waals forces). This confirms the presence of polar groups on the surface.
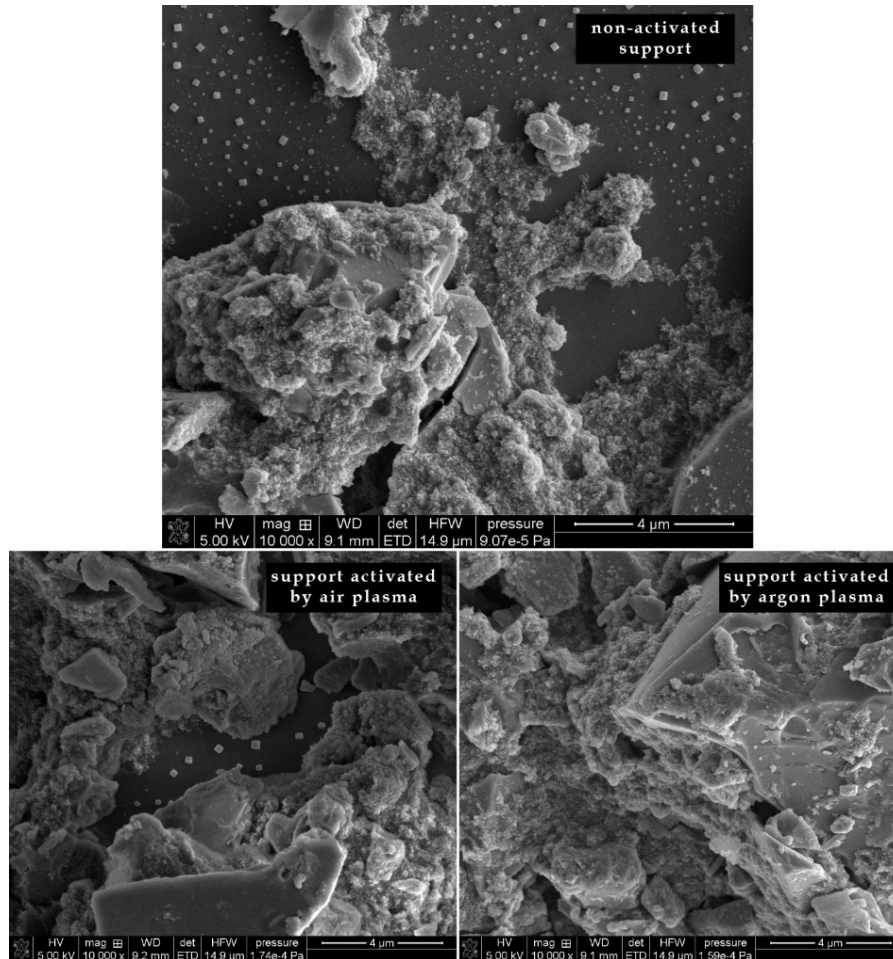
Fig. 7. The SEM images of the obtained surfaces

Table 2. Quantitative and qualitative compositions of the surfaces obtained via the XPS experiment

Support modification	Si (at. %) 2p	C (at. %) 1s	O (at. %) 1s
non-activated	38.23	13.24	48.36
argon plasma	37.84	11.31	50.58
air plasma	34.73	16.3	48.74

Table 3. The surface free energies of the coatings calculated by the CAH method

Support modification	Surface free energy $\left(\frac{mJ}{m^2}\right)$
non-activated	4.0 ± 0.9
argon plasma	3.4 ± 1.2
air plasma	7.3 ± 1.3

4. Conclusions

Hydrophobic coatings on the plasma activated glass supports were fabricated using the dip-coating method and doped silica gel obtained by the sol–gel process with TEOS as the precursor. Water contact angle measurements showed that the obtained layers are highly hydrophobic (WCA > 120°). The microscale roughness of the layers was confirmed by the optical profilometry. FTIR-ATR, FTIR/PAS and the XPS spectra confirmed the presence of the hydrophobic methyl groups over the silica surface. However, in the case of the layer deposited on the support activated by air plasma, these techniques highlighted the presence of many oxygen groups. The presence of the polar (hydrophilic) groups was confirmed also by the surface free energy calculations and worse wettability was observed. For this reason, the support activation by air plasma did not improve the hydrophobicity of the deposited coating while in the case of argon plasma hydrophobicity an increase was observed. Due to their properties, these coatings can be useful in construction of anti-wetting artificial surfaces for various practical applications. Moreover, they are a good base for constructing hybrid surfaces.

Acknowledgments

References

ARASE, H., TANIGUCHI, K., KAI, T., MURAKAMI, K., ADACHI, Y., OOYAMA, Y., KUNUGI, Y., OHSHITA, J., 2019. *Hydrophobic modification of SiO₂ surface by aminosilane derivatives*. Compos. Interface. 26, 15-25.

BOGUSH, G.H., TRACY, M.A., ZUKOSKI, C.F., 1988. *Preparation of monodisperse silica particles: Control of size and mass fraction.* J. Non-Cryst. Solids 104, 95-106.

CHIBOWSKI, E., 2003. *Surface free energy of a solid from contact angle hysteresis*. Adv. Colloid Interface Sci. 103, 149-172.

CHIBOWSKI, E., 2007. *On some relations between advancing, receding and Young's contact angles*. Adv. Colloid Interface Sci. 133, 149-172.

INNOCENZI, P., 2016. *The Sol to Gel Transition*, Springer, Alghero, Italy.

ITO, R., MORISATO, K., KANAMORI, K., NAKANISHI, K., 2019. *Preparation of surface-coated macroporous silica (core-shell silica monolith) for HPLC separations*. J. Sol-Gel Sci. Technol. 90, 105-112.

JIANG, C., LIU, W., SUN, Y., LIU, C., YANG, M., WANG, Z., 2019. *Fabrication of durable superhydrophobic and superoleophilic cotton fabric with fluorinated silica sol via sol-gel process*. J. Appl. Polym. Sci. 136, 47005.

LI, Y., HE, J., ZHANG, K., LIU, T., HU, Y., CHEN, X., WANG, C., HUANG, X., KONG, L., LIU, J., 2019. *Super rapid removal of copper, cadmium and lead ions from water by NTA-silica gel*. RSC Adv. 9, 397-407.

LIN, D., ZENG, X., LI, H., LAI, X., WU, T., 2019. *One-pot fabrication of superhydrophobic and flame-retardant coatings on cotton fabrics via sol-gel reaction*. J. Colloid Interf. Sci. 533, 198-206.

McDONAGH, C., SHERIDAN, F., BUTLER, T., MACCRAITH, B.D., 1995. *Characterisation of sol-gel-derived silica films*. J. Non-Cryst. Solids 194, 72-77.

McHALE, G., SHIRTCLIFFE, N.J., NEWTON, M.I., 2004. *Contact-angle hysteresis on super-hydrophobic surfaces*. Langmuir 20, 10146-10149.

MILEA, C.A., BOGATU, C., DUTA, A., 2011. *The influence of parameters in silica sol-gel process*. Bull. Trans. Univer. Braşov, ser. I: Eng. Sci. 4, 59-66.

PALLA-RUBIO, B., ARAÚJO-GOMES, N., FERNÁNDEZ-GUTIÉRREZ, M., ROJO, L., SUAY, J., GURRUCHAGA, M., GOÑI, I., 2019. *Synthesis and characterization of silica-chitosan hybrid materials as antibacterial coatings for titanium implants*. Carbohydr. Polym. 203, 331-341.

KLONOS, P.A., GONCHARUK, O.V., PAKHLOV, E.M., STERNIK, D., DERYŁO-MARCZEWSKA, A., KYRITSIS, A., GUN'KO, V.M., PISSIS, P., 2019. *Morphology, molecular dynamics, and interfacial phenomena in systems based on silica modified by grafting polydimethylsiloxane chains and physically adsorbed polydimethylsiloxane*. Macromolecules 52, 2863-2877.

PIERRE, A.C., 2019. *From random glass networks to random silica gel networks and their use as host for biocatalytic applications*. J. Sol-Gel Sci. Techn. 90, 172-186.

PISCITELLI, F., TESCIONE, F., MAZZOLA, L., BRUNO, G., LAVORGNA, M., 2019. *On a simplified method to produce hydrophobic coatings for aeronautical applications*. Appl. Surf. Sci. 472, 71-81.

PONAMOREVA, O.N., LAVROVA, D.G., KAMANINA, O.A., RYBOCHKIN, P.V., MACHULIN, A.V., ALFEROV, V.A., 2019. *Biohybrid of methylotrophic yeast and organically modified silica gels from sol–gel chemistry of tetraethoxysilane and dimethyldiethoxysilane.* J. Sol-Gel Sci. Techn., 1-8 (https://doi.org/10.1007/s10971-019-04967-8).

PROTSAK, I., TERTYKH, V., PAKHLOV, E., DERYLO-MARCZEWSKA, A., 2017. *Modification of fumed silica surface with mixtures of polyorganosiloxanes and dialkyl carbonates.* Prog. Org. Coat. 106, 163-169.

PROTSAK, I.S., GUN'KO, V.M., HENDERSON, I.M., PAKHLOV E.M., STERNIK, D., LE, Z., 2019. *Nanostructured amorphous silicas hydrophobized by various pathways.* ACS Omega 4, 13863-13871.

STÖBER, W., FINK, A., BOHN, E., 1968. *Controlled growth of monodisperse silica spheres in the micron size range.* J. Colloid Interf. Sci. 26, 62-69.

SULEJMANOVIĆ, J., ŠABANOVIĆ, E., BEGIĆ, S., MEMIĆ, M., 2018. *Molybdenum(VI) oxide-modified silica gel as a novel sorbent for the simultaneous solid-phase extraction of eight metals with determination by flame atomic absorption spectrometry.* Anal. Lett. 52, 588-601.

WANG, Z., YANG, W., SUN, F., ZHANG, P., HE, Y., WANG, X., LUO, D., MA, W., GONZALEZ-CORTES, S., 2019. *Construction of a superhydrophobic coating using triethoxyvinylsilane-modified silica nanoparticles.* Surf. Eng. 35, 418-425.

ZHAO, Y., LI, J., HU, J., SHU, L., SHI, X., 2011. *Fabrication of super-hydrophobic surfaces with long-term stability.* J. Dispers. Sci. Technol. 32, 969-974.

ZHI, D., WANG, H., JIANG, D., PARKIN, I.P., ZHANG, X., 2019. *Reactive silica nanoparticles turn epoxy coating from hydrophilic to super-robust superhydrophobic.* RSC Adv. 9, 12547-12554.